Mapping the influence of the gut microbiota on small molecules across the microbiome gut brain axis

Heather Hulme[1], Lynsey M. Meikle[1], Nicole Strittmatter[2], John Swales[2], Gregory Hamm[2], Sheila L. Brown[3], Simon Milling[1], Andrew S. MacDonald[3], Richard J.A. Goodwin[2], Richard Burchmore[1], Daniel M. Wall[1,*]

[1]Institute of Infection, Immunity and Inflammation, College of Medical, Veterinary and Life Sciences, Sir Graeme Davies Building, University of Glasgow, Glasgow G12 8TA, United Kingdom

[2]Imaging and Data Analytics, Clinical Pharmacology and Safety Sciences, Biopharmaceuticals R&D, AstraZeneca, Cambridge, CB4 0WG, UK

[3]Lydia Becker Institute of Immunology and Inflammation, Faculty of Biology, Medicine and Health, Manchester Academic Health Science Centre, University of Manchester, Manchester M13 9NT, UK

*Corresponding author email: Donal.Wall@glasgow.ac.uk

*Corresponding author address:

Dr. Daniel (Dónal) M. Wall

Institute of Infection, Immunity and Inflammation

College of Medical, Veterinary and Life Sciences

Sir Graeme Davies Building

University of Glasgow

120 University Place

Glasgow G12 8TA

Keywords: mass spectrometry imaging, microbiome, brain, neurotransmitters, metabolites

Abstract

Microbes exert influence across the microbiome-gut-brain axis through neurotransmitter production, induction of host immunomodulators, or through the release or induction of other microbial or host molecules. Here we used mass spectrometry imaging (MSI), a label-free imaging tool, to map molecular changes in the gut and brain in germ-free, antibiotic-treated and control mice. We determined spatial distribution and relative quantification of neurotransmitters and their precursors in response to the microbiome. Using untargeted MSI we detected a significant change in the levels of four identified small molecules in the brains of germ-free animals compared to controls. However, antibiotic treatment induced no significant changes in these same metabolites in the brain after one week of treatment. This work exemplifies the utility of MSI as a tool for the study of known, and discovery of novel, mediators of microbiome-gut-brain axis communication.

Introduction

Deciphering the complex bi-directional communication across the microbiome gut brain (MGB) axis remains a challenging prospect. The composition and stability of the gut microbiome is now proposed to be a significant contributor to human health with changes in its composition suggested as a contributing factor in a number of neurological conditions. Diverse human neurological disorders, ranging from autism spectrum disorders (ASDs) and attention-deficit/hyperactivity disorder (ADHD) to Alzheimer's and Parkinson's disease, have linked gastrointestinal abnormalities or changes in the gut microbiome (*1*–*6*). Similarly, altered levels of certain bacterial species in the gut have been linked with depression (*7*, *8*).

Despite the deficiencies of germ free (GF) animal models, their use for investigating links between the gut microbiota and the brain have proved informative and are helping to uncover the influence of bacteria on neurotransmitter levels alongside other bacterial and host metabolites. Their neuro-developmental abnormalities including increased blood-brain-barrier (BBB) permeability, alterations in abundance and maturity of microglia cells, and reduced myelination (*9*–*11*) have been well documented but their use, alongside antibiotic treated (ABX) mice, have provided further evidence that supports the importance of a stable and healthy gut microbiota in maintaining normal cognitive function and development (*12*). GF mice display reduced anxiety-like behaviour and an increased response to stress that is fully alleviated upon colonisation with *Bifidobacterium infantis* (*12*–*15*), while murine ABX treatment models reinforce the significance of the MGB axis with treated mice showing impaired cognition and significantly altered behaviours that can be linked to absence of particular bacteria (*16*–*19*). These effects are likely mediated by the numerous bacterial molecules including short chain fatty acids (SCFAs), phenolic acids, quorum sensing peptides, peptidoglycan and lactic acid, that have been proposed to exert influence across the MGB axis (*20*–*22*). SCFAs both cross and modulate the permeability of the BBB, while animals and humans are also dependent on intestinal microbes to produce or supplement their vitamin needs (*10*, *23*, *24*).

Signalling across the MGB axis can occur via the vagus nerve, bacterial modulation of host immune responses or host neurotransmitter production, and signalling through bacterial neurotransmitters or other microbial molecules. Microbes produce a number of neurotransmitters including gamma aminobutyric acid (GABA), norepinephrine and dopamine, serotonin, and acetylcholine, while bacterial production or depletion of essential neurotransmitter intermediates such as tryptophan can also affect host production (*14*, *19*, *25*–*30*). Manipulation of the microbiome can also alter host neurotransmitter levels as microbes stimulate their intestinal production, with depletion of the microbiome or its supplementation with probiotic bacteria, capable of altering specific levels of neurotransmitters even in the brain (*31*–*35*).

Understanding how the gut microbiota influence the brain, and the complex network of molecules and neurotransmitters that mediate this influence, is a significant challenge requiring novel tools and approaches. Mass spectrometry imaging (MSI) is a molecular imaging tool that can be applied to understand and map biological systems with recent successes in mapping microbial interactions with their environment (*36*–*38*). MSI maps the distribution of small molecules across a tissue section independent of any label, so no prior knowledge of the molecules present is required. The ability to detect spatial distribution and abundance of thousands of compounds simultaneously in tissue sections makes this a powerful approach for studying the MGB axis. Here, using MSI, we detected significant differences in neurotransmitter levels and those of their precursors in the guts of both GF and ABX mice. However, in the brain only tryptophan levels were significantly affected in ABX treated mice compared to controls, with significant changes detected in every brain region imaged. Through untargeted MSI we also discovered four small molecules that were significantly changed in the GF brain. We focused on two of these, identified as 3-hydroxy-3-methylglutaric acid (3-HMG) and pantothenic acid (vitamin B5). 3-HMG, a metabolite associated with oxidative stress, was significantly increased in the GF brain, while vitamin B5, which can be produced by the microbiome, was present at a

lower level in GF brain and is implicated in brain health. This work indicates that the brain remains largely protected from microbiome changes in the gut and indicates plasticity, not just in the brain, but across the MGB axis in GF mice.

Methods

Animal models used in this study

Germ-free studies

All germ-free (GF) work was undertaken at the University of Manchester Gnotobiotic Facility. Five GF and specific pathogen free (SPF) mice were used in this study, which were male mice, aged 7-8 weeks, on a C57BL/6J background strain. Both experimental groups were fed the same pelleted diet that was irradiated with 50 kGy to ensure sterility. The Manchester Gnotobiotic Facility was established with the support of the Wellcome Trust (097820/Z/11/B), using founder mice obtained from the Clean Mouse Facility (CMF), University of Bern, Bern, Switzerland.

Antibiotic studies

All work involving antibiotic (ABX) treatment was undertaken at the University of Glasgow. Five ABX treated animals and corresponding untreated controls were used in these studies and were male mice, aged 7-8 weeks, on a C57BL/6J background strain. The ABX cocktail consisted of 1 mg/ml gentamicin, 1 mg/ml neomycin and 0.5 mg/ml vancomycin in sterile distilled drinking. ABX supplemented drinking water was provided ad libitum for a period of 1 week and refreshed every 2 days. The untreated controls were given sterile drinking water without ABXs ad libitum, which again was refreshed every two days. Both treated and control groups were fed the same standard chow. All antibiotics selected for this study were chosen based on their specificity for the gut microbiota; to the best of our knowledge the antibiotics used are not absorbed by the intestine. Approval for these procedures was given prior to their initiation by internal University

of Manchester and University of Glasgow ethics committees and by the U.K. Home Office under licenses 70/7815, PPL40/4500, P64BCA712 and P78DD6240.

Tissue processing

Mice were culled by cervical dislocation and brains and colons were removed. Brains were placed in a mould and were immediately frozen using a slurry of dry-ice and ethanol to maintain structural integrity and to ensure that all biochemical processes were halted. The colon samples were then cut lengthwise over ice and the faecal matter was removed and the remaining GI tissue was then rolled using the 'Swiss roll technique' before embedding in 2.5% medium viscosity carboxymethyl cellulose (Sigma-Aldrich, Dorset, UK). Both brains (in sagittal orientation) and colons were sectioned using a CM3050S cryostat microtome (Leica Biosystems, Nussloch, Germany) to 10 µm thickness at -18°C. Colon and brain sections were either thaw mounted onto indium tin oxide (ITO) coated slides for Matrix Assisted Laser Desorption/Ionization (MALDI)-MSI or normal microscope slides for desorption electroSpray ionisation (DESI)-MSI. Tissue sections from the different conditions were randomly located on each slide and the slides run in different orientations. Each slide contained sections from both conditions that were being compared, for example, both GF and SPF sections were mounted on the same slide and imaged in the same mass spectrometer experiment. This was to ensure the sections from the different conditions were prepared identically and to control for any possibility of artefacts occurring during derivatization agent spraying or due to variation in mass spectrometer signal across the slide. For the brain, stereotactically matched sections were selected to ensure that all comparisons were performed using corresponding brain regions. Consecutive sections to those for MSI were collected for histology purposes. Slides were prepared and stored at -80°C until required for analysis. Prior to derivatisation, matrix application or analysis, the slide was taken from -80°C and brought to room temperature under a stream of air.

144

145 ***Neurotransmitter derivatisation***

146 The derivatisation of primary amine neurotransmitters was performed as previously described
147 (*39*). Nine milligrams of 2,4-diphenyl-pyranylium tetrafluoroborate (DPP-TFB) was added to 1.2
148 mL of 100% methanol and sonicated for 20 minutes (min). This was then gradually added to 6
149 mL of 70% methanol in water with 3.5 µL of trimethylamine. This solution was sprayed onto the
150 tissue for derivatisation using an automated sprayer (TM-Sprayer, HTX Technologies); 30
151 passes were performed using a nozzle temperature of 75°C, velocity of 1100 mm/min, flow rate
152 of 80 µL/min, and gas pressure of 6 psi. After coating, the slide was incubated in a petri dish
153 with vapour from a 50 % methanol/water solution 3 times for 5 min each.

154

155 ***DESI-MSI analysis***

156 DESI-MSI was performed on a Q-Exactive mass spectrometer (Thermo Scientific, Waltham,
157 MA, US) equipped with an automated 2D DESI source (Prosolia Inc, Indianapolis, IN, USA). A
158 home-built DESI sprayer assembly, as described previously (*40*), was used with the spray tip
159 positioned at 1.5 mm above the sample surface and at an angle of 75°. The distance between
160 the sprayer to mass spectrometer inlet was 7 mm with a collection angle of 10° and <1mm
161 distance between inlet and sample surface. The spray solvent was methanol/water (95:5 *v*/*v*),
162 delivered at 1.5 µL/min using a Dionex Ultimate 3000 pump (Thermo Scientific, Waltham, MA,
163 US) at a spray voltage of ±4.5 kV. Nitrogen was used as the nebulisation gas at a pressure of 7
164 bars. General instrument settings used to image specific molecules are shown in Table 1. For
165 acquisition of MS/MS spectra, an injection time of 300 ms, mass resolution of 70000 and a
166 mass isolation window of ± 0.3 Da was used. For MS/MS imaging of metabolites with mass to
167 charge (*m/z*) ratios 161.044 and 218.103, various fragmentation Higher Collision induced
168 Dissociation (HCD) settings were used, at a spatial resolution of 100 µm.

Data was recorded as individual line scans and converted into imzML format using imzML converter version 1.1.4.5 (*41*) and visualised using MSiReader version 0.09 (*42*). Imaging data from analysis of the brains was normalized by total ion count due to ion suppression effects in different areas of the brain, data from analysis of colons was not normalized. First order linear interpolation was used for image generation. All mean intensities of the molecules of interest were determined across the entire tissue section or brain region analysed. Brains were divided into regions for relative quantitation of neurotransmitters and metabolites. Major regions were annotated according to the Allen sagittal mouse brain atlas; the cortex (cor), hippocampus (hipp), Hypothalamus (hyp), thalamus (thal), striatum (stri), midbrain (mid), pons, medulla (med), white matter of the cerebellum (Cb white), grey matter of the cerebellum (Cb grey) and the corpus callosum (cc) (*43*, *44*). The substantia nigra (SN) was also imaged due to high abundance of neurotransmitters such as dopamine and serotonin found in this area. An annotated H and E stain of a brain depicting the brain regions is shown in Supplementary Fig. 1. The mean intensity was used to normalize by the area of the region analyzed, which controls for any difference in size of the tissue sections or regions between mice. Relative quantitation was performed on the most abundant peak in the mass spectrum for each metabolite. For all derivatized neurotransmitters and the metabolite at *m/z* 161.044, only the [M+H]+ ion was detected. For the metabolite at *m/z* 218.103, both the [M-H]- and [M+Cl]- ions were detected, however, the [M+Cl]- was very low abundance and not detected in some brain regions, therefore, the [M-H]- was used for relative quantitation as it would be more accurate (Supplementary Fig. 2). The data from the colons was transformed to log10 prior to statistical analysis, the relative abundance values for the brain were not transformed. A Shapiro-Wilk normality test was performed on the data to check for a normal distribution. If the data passed the normality test an unpaired t-test was performed. If the data failed the test a Mann-Whitney U test was performed. When biological replicates were analysed over two separate DESI-MSI experiments a paired t-test was performed instead.

H&E staining of brains and colons

Brain and colon sections that had undergone MSI analysis were H and E stained post-imaging to permit localisation of candidate metabolites and neurotransmitters to specific brain regions. Sections were fixed on the slide in ice cold 75% acetone and 25% ethanol for 10 min, and air dried for a further 10 min. Slides were placed in water for 2 min, submerged in haematoxylin (Sigma-Aldrich, Poole, Dorset, UK) for 2 min and immediately rinsed in cold running water. The slides were then dipped for 3 sec in acid alcohol 0.5% (Atom Scientific Hyde, Cheshire, UK), and rinsed in water before submerging in Scott's tap water (Atom Scientific Hyde, Cheshire, UK) for a further 30 sec. The sections were counter-stained with eosin (Sigma Aldrich, Poole, Dorset, UK) for 2 min and washed in water. Sections were then dehydrated in increasing concentrations of ethanol (70 % ethanol for 30 sec, 90 % for 1 min, and twice for 3 min in 100 % ethanol), cleared in xylene (twice for 3 min), and cover slipped using DPX mounting media (Atom Scientific, Hyde, Cheshire, UK).

Results

Targeted neurotransmitters remain unaffected by the lack of a gut microbiota

The brains and colons from germ free (GF) and conventionally colonized, specific pathogen free (SPF) control mice were first compared by MSI using a targeted approach. DPP-derivatisation of primary amines was performed to allow targeted imaging of neurotransmitters, neurotransmitter precursors and neurotransmitter metabolites; serotonin, tryptophan, dopamine, tyrosine, 3-methoxy-tyramine, GABA and glutamate (Fig. 1a-b) (*39*, *45*, *46*). Significant differences in the levels of several neurotransmitters were observed in the gut. Serotonin was lower (3.8-fold decrease) in the GF mouse gut (Fig. 1b; $P \leq 0.01$), whilst glutamate (1.3-fold increase) (Fig. 1b; $P \leq 0.05$) and the dopamine precursor tyrosine (1.8-fold increase) (Fig. 1b; $P \leq 0.01$) were significantly increased in the GF gut. There were no differences detected in the levels of tryptophan, dopamine, 3-methoxy-tyramine or GABA in the gut of GF mice (Supplementary Fig. 3). Changes in serotonin, glutamate and tyrosine levels in the intestine were not reflected in the corresponding brain sections of GF mice where no significant differences were identified for any of the seven neurotransmitters or their precursors across whole brain sections (Fig. 1a). Targeted MSI of specific brain regions (cortex, hippocampus, hypothalamus, thalamus, striatum, midbrain, substantia nigra, pons, medulla, white matter cerebellum, grey matter cerebellum, corpus callosum) was undertaken to further investigate these findings further but no significant change was seen in the targeted neurotransmitters or precursors in any region of the GF mouse brain when compared to the corresponding region in control mice (Fig.1a).

MSI of neurotransmitters in the brains and colons of ABX treated mice

To determine whether an acute disruption of the microbiota over 7 days could have an influence on the levels or the localisation of the same neurotransmitters in the brain, the colon and the brains of ABX treated mice were imaged in a targeted manner.

Tyrosine levels were changed in ABX treated mice in a manner similar to that seen in GF mice with a significant increase in the colon (2.2-fold), but again this intestinal increase in tyrosine levels was not reflected in levels of tyrosine across whole brain sections (Fig. 1c-d). Unlike GF mice, ABX treated mice showed no significant change in the levels of serotonin, in either the colon or brain, compared to untreated mice (Supplementary Fig. 4). However, there was significantly higher abundance of tryptophan in both the colon (3.2-fold; $P \leq 0.05$) and brain (1.7-fold; $P \leq 0.01$) of ABX treated mice compared to controls (Fig. 1c-d). Imaging of individual brain regions indicated that tryptophan levels were significantly increased in each individual region in the ABX mice in comparison to control mice, with the highest fold changes observed in the corpus callosum (2.1-fold), the midbrain (2.1-fold), and the substantia nigra (2-fold). Dopamine levels were also significantly higher (3.3-fold; $P \leq 0.001$) in the colons from ABX treated mice compared to untreated, but no significant change was detected across the whole brain or in the striatum or substantia nigra, where dopamine was most abundant (Fig. 1d). No significant difference was detected in levels of 3-methoxytyramine, glutamate or GABA in either the gut or brain sections imaged (Supplementary Fig. 4).

Untargeted MSI to detect novel molecular changes in GF mouse brains

As no significant changes were seen in several neurotransmitters in GF brains, untargeted imaging was performed using DESI-MSI on the colon and brains of GF mice to probe the MGB axis for molecular changes induced by microbiota disruption. Full scan spectra were collected from *m/z* 65-400 and *m/z* 250-1000, in both positive and negative ionisation mode, allowing detection of a wide range of metabolites and not targeted towards a particular group. Significant differences were detected in only three masses when comparing GF and SPF mouse brains. Two of these identified metabolites at *m/z* of 218.1030 and *m/z* 161.0446, both detected in negative ion mode, were selected for further analysis as putative identities could be assigned from online databases, as discussed further below. The third mass at *m/z* 160.133 was below

the limit of detection in GF brains and could not be assigned an identity from online databases. The identity of this mass as two microbiome-derived metabolites of identical elemental composition, 3-methyl-4(trimethylammonia)butanoate and 4-(trimethylammonio)pentanoate), was finally determined via two-dimensional NMR after isolating the producing bacterial species, with the associated structures and their bacterial origin recently described (*47*).

Levels of 3-hydroxy-3-methylglutaric acid (3-HMG –m/z 161.0446) are increased in the GF brain

The molecule detected at *m/z* 161.0446 in negative ionisation mode, was found at significantly higher levels ($P \leq 0.0001$) across the whole brain section of GF compared to SPF mice, with levels significantly higher in the grey and white matter of the cerebellum (10-fold and 7-fold respectively) (Fig. 2a). The change in the brain was not reflected in the gut as levels in the colon did not significantly change between GF and SPF control mice (Fig. 2b). The metabolite was identified as [M-H]- of 3-hydroxy-3-methylglutaric acid (3-HMG) through searching the Human Metabolome Database (*48*, *49*) and then confirmed using tandem mass spectrometry (MS/MS) analysis and comparison to an HMG standard (Supplementary Fig. 5). No significant difference in abundance of HMG was found in brains and colon after ABX treatment compared to controls (Fig. 2c-d).

Quantification analysis of HMG revealed an average concentration of 0.56 µg/g of tissue in the GF brain compared to <0.01 µg/g of tissue in the SPF brain (Supplementary Figure 6). The concentration of HMG was particularly high in the cerebellum in the GF mouse brain at a concentration of 5.02 µg/g of tissue compared to <0.01 µg/g of tissue in the SPF mouse brains.

Vitamin B5 (m/z 218.1030) levels are decreased in the brain of GF mice

The second of the unknown molecules had an *m/z* of 218.1030 in negative ionisation mode and was found to be significantly lower in the brain of GF mice compared to SPF controls (Fig. 3a; *P*

≤0.05). This difference was most obvious in the grey and white matter of the cerebellum (1.6-fold and 1.9-fold respectively), the hypothalamus (1.7-fold) and the thalamus (1.7-fold). This molecule was unchanged between GF and SPF colons. The metabolite was identified as [M-H]- of pantothenic acid, also known as vitamin B5, through a database search and subsequent confirmatory MS/MS analysis (Supplementary Fig. 7).

No difference was found in the levels of vitamin B5 in the brain or colon in ABX treated mice compared to untreated control mice (Fig. 3a and 3b). Quantification analysis of vitamin B5 revealed an average concentration of 0.25 µg/g of tissue in the GF brain compared to 0.36 µg/g of tissue in the SPF brain (Supplementary Fig. 8).

Discussion

Studying the MGB axis has significant potential to help us understand and potentially treat, via the microbiome, certain neurological conditions. However, in order to achieve this goal a greater understanding of MGB communication is required. The techniques applied to date to discover mediators of communication across the MGB axis have typically been targeted toward specific neurotransmitters, metabolites or regions of the brain (*14*, *19*, *26*). Such approaches are often dependent on analyte extraction from brain tissue prior to analysis, meaning data regarding spatial localisation within the brain was limited. Here we applied MSI to study the metabolic processes along the MGB axis, permitting imaging of multiple neurotransmitters in the presence and absence of a microbiome while untargeted MSI also allowed the discovery of novel metabolites involved in MGB axis communication.

Serotonin, tryptophan, dopamine, tyrosine, 3-methoxytyramine, GABA and glutamate were first imaged to detect changes across the brain and gut of GF animals. No changes were detected when imaging levels of each across whole brain sections whilst in the intestine only tyrosine and glutamate were increased, and serotonin decreased in GF animals compared to SPF controls. Significantly lower levels of serotonin have previously been detected in the colon of GF mice

along with increased levels of the serotonin precursor tryptophan (*32*). No difference in serotonin or tryptophan levels were detected in the brain of GF compared to SPF mice in contrast to previous GF work focused on these neurotransmitters (*14*, *50*). One week antibiotic (ABX) treated mice were also tested for changes in levels of serotonin and tryptophan in the gut and brain compared to untreated controls. Tryptophan abundance increased in both the colon and the brain of ABX treated mice compared to untreated controls, but serotonin levels remained unchanged. Tryptophan levels were seen to increase significantly in every brain region imaged in ABX mice. This data mirrors that previously obtained with a similar model, where ABX treatment increased systemic tryptophan whilst serotonin levels remained unaffected (*19*, *34*).

Data comparison between microbiome studies is complex with prior studies employing rat or mouse models as well as different experimental tools, while also highlighting that differences in these molecules can be sex-specific, complicating comparison with our own data. Whilst microbiome changes within mouse colonies as well as between mouse strains are well documented, phenotypic comparisons between GF rodent models which lack a microbiome have also been limited (*51–53*).

Dopamine and its precursor tyrosine were also affected by microbiota disruption or absence. Increased tyrosine and dopamine levels were detected in the colon in ABX treated mice while GF mice had increased intestinal tyrosine levels compared to controls. Yet no difference was found in the abundance of either of these molecules in the brains of GF or ABX mice, with no single specific brain region determined to have significantly changed levels of either molecule. Previous work found a decrease in the level of dopamine in the guts of GF mice, whilst another found no difference in the levels of dopamine in the colon after ABX treatment, although antibiotic treatments varied by constitution and duration between ours and previous studies (*16*, *28*). As tyrosine can be metabolized by certain bacterial species, it is possible that in addition to causing increased tyrosine levels, reduction in these groups could lead to higher production of

dopamine (*54*). Conversely the release of a biologically active free form of dopamine in the gut, via bacterial β-glucuronidase mediated breakdown of a conjugated form of dopamine, could also play a significant role (*28*). Additionally, although there are no differences in the levels of dopamine in the brain, increased levels in the colon could have localised effects. There are dopamine receptors present in the intestine and dopamine, in a similar manner to serotonin, has been shown to increase water absorption from the gut and regulation of muscle contraction (*28*, *55*, *56*).

The neurotransmitter, and GABA precursor, glutamate was increased in the colon of GF mice compared to controls. Glutamate and GABA are the main excitatory and inhibitory neurotransmitters of the central nervous system, respectively (*57*). The increase in glutamate levels in GF mice was surprising given the number of bacteria known to produce glutamate in the intestine (*58*). This build-up of glutamate is not due to reduced conversion to GABA as we detected no corresponding difference in GABA levels (*59*). No increase in glutamate in the GF brain was detected in these GF mice with high intestinal glutamate levels, but glutamate is primarily metabolised in the splanchnic area and little enters into circulation from the gastrointestinal tract, instead exerting its significant localised effects on the gut including through stimulation of the vagus nerve (*60*, *61*).

Untargeted MSI indicated that four metabolites were significantly altered in the brain, vitamin B5 or pantothenic acid (*m/z* 218.1030), 3-hydroxy-3-methylglutaric acid (3-HMG; *m/z* 161.0446) and *m/z* 160.133. The latter *m/z* was determined to be a mixture of two metabolites which are discussed in detail elsewhere (*47*). Vitamin B5 was significantly decreased in GF mice compared to SPF, whereas 3-HMG was increased. Further analysis of vitamin B5 and HMG determined that they were not significantly altered in ABX treated mice. Vitamin B5 is a precursor for co-enzyme A, which is a critically important molecule in many metabolic pathways including neurotransmitter biosynthesis, the TCA cycle and metabolism of fatty acids, protein, RNA and histones (*62*, *63*). Previously it was thought that only small amounts of vitamin B5

366 could be produced by the microbiota but recent work identified a previously uncharacterised
367 group of *Clostridia* that harbour genes for pantothenic acid biosynthesis (*64*, *65*). It has also
368 recently been determined that levels of vitamin B5 producing bacteria change according to
369 gestational age in preterm infants (*65*). Neurological symptoms of vitamin B5 deficiency were
370 determined in early studies by inducing deficiency in human subjects, which resulted in defects
371 in neuromuscular function and deterioration of mood (*66*). Vitamin B5 deficiency is observed in
372 the human brain across a number of neurodegenerative conditions including Parkinson's
373 disease (PD), Alzheimer's disease (AD) and Huntington's disease (HD) (*63*, *67*, *68*). The lower
374 levels in the GF mouse brain were particularly apparent in the cerebellum, hippocampus and
375 hypothalamus regions and these decreased levels mirrored those detected in the cerebellum of
376 HD, AD and PD patients, and hippocampus of HD and AD patients (*63*, *67*, *68*). Despite the
377 potential for a microbial origin for vitamin B5, no change was found in the levels of vitamin B5 in
378 the colons of GF mice making it unclear what role, if any, the microbiota may play in the
379 significant decrease in vitamin B5 levels in the brain. Vitamin B5 crosses into the brain through
380 the BBB via a saturable transporter and levels are maintained in the brain at around 50 times
381 the concentration found in the plasma, meaning that any reduction in microbiota-derived vitamin
382 B5 levels may require more prolonged antibiotic treatment before effects are seen (*10*, *69*, *70*).
383 HMG, a metabolite involved in leucine degradation and ketogenesis was present at higher
384 levels across the brains of GF mice compared to normal brains, but particularly in the
385 cerebellum. Individuals with the genetic disorder 3-hydroxy-3-methylglutaric aciduria, which
386 leads to a build-up of metabolites including HMG, suffer from neurological symptoms including
387 seizures and abnormalities in the brain (*71*). It has been proposed that this accumulation of
388 metabolites is directly affecting the brain with HMG inducing oxidative damage (*71–74*). The
389 particularly high levels of HMG in the cerebellum, a brain region involved in motor control,
390 suggests this region would be most affected in the GF mice. Histopathology analysis of a cat
391 brain with HMG accumulation, due to 3-hydroxy-3-methylglutaric aciduria, showed cerebellum

changes along with changes in gait (*75*). While gait changes in GF mice have not been reported, increased motor activity compared to control mice has been reported (*12*). Presence of HMG in the serum has been associated with increased gut permeability in children with environmental enteric dysfunction (*76*). Studies have shown that bacteria play a role in maintaining intestinal barrier function, therefore, the increased intestinal permeability seen in the GF intestine could be leading to higher levels of HMG in circulation compared to normal mice (*77*). Furthermore, intraperitoneal injections of HMG into rats leads to high levels accumulating in the brain of 7 day old rats but not in 30 day old rats in what was speculated to be a BBB permeability related effect (*71*). It has been demonstrated that BBB tight junction proteins such as claudin-5, levels of which are decreased in the absence of a gut microbiota, are essential for BBB function and their absence increases permeability to small molecules (*10*, *78*). Therefore, given the intestinal permeability defects and the size selective permeability in the BBB in GF mice, HMG and other small metabolites, are likely entering the circulation and subsequently the brain at higher levels (*10*). Furthermore, no significant difference was found in the levels of HMG in the brain of ABX treated mice where such BBB defects have not been described.

Conclusions:

This study has highlighted the capabilities and potential of MSI to enhance investigation of the MGB axis through the detection and discovery of molecules involved in MGB communication. Here we show that, despite significant changes in gut microbiota, neurotransmitters are not significantly changed in the brain. As the significance of the MGB axis is still being realised, MSI offers a unique opportunity to understand the complexity of these interactions by identifying both the known and unknown mediators of host-microbe communication.

Associated content

Supporting information

Supplementary methods: MALDI-MSI analysis; 3-hydroxy-3-methylglutaric acid (HMG) and pantothenic acid (vitamin B5) quantitation. Supplementary figures: Fig. S1, brain annotations; Fig. S2, pantothenic acid detected ions; Fig. S3, Effects of the gut microbiome on neurotransmitters, neurotransmitter precursors and neurotransmitter metabolites in the murine brain and gut; Fig. S4, Effects of the gut microbiome on neurotransmitters, neurotransmitter precursors and neurotransmitter metabolites in the murine brain and gut (post-ABX treatment); Fig. S5, Identification of metabolite at *m/z* 161.0446; Fig. S6, Absolute quantification of HMG in GF and SPF brain; Fig. S7, Identification of the metabolite at *m/z* 218.102; Fig. S8, Absolute quantification of vitamin B5 in GF and SPF brain.

Author information

Daniel M. Wall Institute of Infection, Immunity and Inflammation, College of Medical, Veterinary and Life Sciences, University of Glasgow, Glasgow, G12 8QQ, United Kingdom.

https://orcid.org/0000-0002-0421-1951 **E-mail:** donal.wall@glasgow.ac.uk

Authors' contributions

The manuscript was written through contributions of all authors. All authors have given approval to the final version of the manuscript.

Declarations

Ethics approval and consent to participate

Approval for animal procedures was given prior to their initiation by internal University of Manchester and University of Glasgow ethics committees and by the U.K. Home Office under licenses 70/7815, PPL40/4500, P64BCA712 and P78DD6240.

Notes

The authors declare that they have no competing interests.

Availability of data and material

The datasets acquired and/or analysed during the current study available from the corresponding author on reasonable request.

Funding

This work was supported by a Biotechnology and Biological Sciences Research Council (BBSRC)-CASE studentship part funded by AstraZeneca to R.B., D.M.W. and R.J.A.G. and BBSRC grants BB/K008005/1 and BB/P003281/1 to D.M.W. The Manchester Gnotobiotic Facility was established with the support of the Wellcome Trust [097820/Z/11/B].

References

1. M. G. Cersosimo, G. B. Raina, C. Pecci, A. Pellene, C. R. Calandra, C. Gutiérrez, F. E. Micheli, E. E. Benarroch, Gastrointestinal manifestations in Parkinson's disease: prevalence and occurrence before motor symptoms. *J. Neurol.* **260**, 1332–1338 (2013).
2. J. B. Adams, L. J. Johansen, L. D. Powell, D. Quig, R. a Rubin, Gastrointestinal flora and gastrointestinal status in children with autism--comparisons to typical children and correlation with autism severity. *BMC Gastroenterol.* **11**, 22 (2011).
3. C. McKeown, E. Hisle-Gorman, M. Eide, G. H. Gorman, C. M. Nylund, Association of Constipation and Fecal Incontinence With Attention-Deficit/Hyperactivity Disorder. *Pediatrics*. **132** (2013).
4. J. H. Wu, Z. Guo, S. Kumar, P. Lapuerta, Incidence of Serious Upper and Lower Gastrointestinal Events in Older Adults with and without Alzheimer's Disease. *J. Am. Geriatr. Soc.* **59**, 2053–2061 (2011).

5. A. Tomova, V. Husarova, S. Lakatosova, J. Bakos, B. Vlkova, K. Babinska, D. Ostatnikova, Gastrointestinal microbiota in children with autism in Slovakia. *Physiol. Behav.* **138**, 179–187 (2015).

6. S. M. Finegold, D. Molitoris, Y. Song, C. Liu, M. Vaisanen, E. Bolte, M. McTeague, R. Sandler, H. Wexler, E. M. Marlowe, M. D. Collins, P. A. Lawson, P. Summanen, M. Baysallar, T. J. Tomzynski, E. Read, E. Johnson, R. Rolfe, P. Nasir, H. Shah, D. A. Haake, P. Manning, A. Kaul, Gastrointestinal Microflora Studies in Late-Onset Autism. *Clin. Infect. Dis.* (2002), doi:10.1086/341914.

7. A. Naseribafrouei, K. Hestad, E. Avershina, M. Sekelja, A. Linløkken, R. Wilson, K. Rudi, Correlation between the human fecal microbiota and depression. *Neurogastroenterol. Motil.* **26**, 1155–1162 (2014).

8. H. Jiang, Z. Ling, Y. Zhang, H. Mao, Z. Ma, Y. Yin, W. Wang, W. Tang, Z. Tan, J. Shi, L. Li, B. Ruan, Altered fecal microbiota composition in patients with major depressive disorder. *Brain. Behav. Immun.* **48**, 186–194 (2015).

9. D. Erny, A. L. Hrabě de Angelis, D. Jaitin, P. Wieghofer, O. Staszewski, E. David, H. Keren-Shaul, T. Mahlakoiv, K. Jakobshagen, T. Buch, V. Schwierzeck, O. Utermöhlen, E. Chun, W. S. Garrett, K. D. McCoy, A. Diefenbach, P. Staeheli, B. Stecher, I. Amit, M. Prinz, Host microbiota constantly control maturation and function of microglia in the CNS. *Nat. Neurosci.* **18**, 965–977 (2015).

10. V. Braniste, M. Al-Asmakh, C. Kowal, F. Anuar, A. Abbaspour, M. Tóth, A. Korecka, N. Bakocevic, L. G. Ng, N. L. Guan, P. Kundu, B. Gulyás, C. Halldin, K. Hultenby, H. Nilsson, H. Hebert, B. T. Volpe, B. Diamond, S. Pettersson, The gut microbiota influences blood-brain barrier permeability in mice. *Sci. Transl. Med.* **6**, 263ra158 (2014).

11. A. E. Hoban, R. M. Stilling, F. J. Ryan, F. Shanahan, T. G. Dinan, M. J. Claesson, G. Clarke, J. F. Cryan, Regulation of prefrontal cortex myelination by the microbiota. *Transl. Psychiatry*. **6**, e774 (2016).

12. R. D. Heijtz, S. Wang, F. Anuar, Y. Qian, B. Bjorkholm, A. Samuelsson, M. L. Hibberd, H. Forssberg, S. Pettersson, Normal gut microbiota modulates brain development and behavior. *Proc. Natl. Acad. Sci.* (2011), doi:10.1073/pnas.1010529108.

13. K. M. Neufeld, N. Kang, J. Bienenstock, J. A. Foster, Reduced anxiety-like behavior and central neurochemical change in germ-free mice. *Neurogastroenterol. Motil.* **23**, 255–265 (2011).

14. G. Clarke, S. Grenham, P. Scully, P. Fitzgerald, R. D. Moloney, F. Shanahan, T. G. Dinan, J. F. Cryan, The microbiome-gut-brain axis during early life regulates the hippocampal serotonergic system in a sex-dependent manner. *Mol. Psychiatry* (2013), doi:10.1038/mp.2012.77.

15. N. Sudo, Y. Chida, Y. Aiba, J. Sonoda, N. Oyama, X. N. Yu, C. Kubo, Y. Koga, Postnatal microbial colonization programs the hypothalamic-pituitary-adrenal system for stress response in mice. *J. Physiol.* (2004), doi:10.1113/jphysiol.2004.063388.

16. P. Bercik, E. Denou, J. Collins, W. Jackson, J. Lu, J. Jury, Y. Deng, P. Blennerhassett, J. MacRi, K. D. McCoy, E. F. Verdu, S. M. Collins, The intestinal microbiota affect central levels of brain-derived neurotropic factor and behavior in mice. *Gastroenterology*. **141**, 599–609 (2011).

17. E. E. Fröhlich, A. Farzi, R. Mayerhofer, F. Reichmann, A. Jačan, B. Wagner, E. Zinser, N. Bordag, C. Magnes, E. Fröhlich, K. Kashofer, G. Gorkiewicz, P. Holzer, Cognitive Impairment by Antibiotic-Induced Gut Dysbiosis: Analysis of Gut Microbiota-Brain Communication. *Brain. Behav. Immun.* (2016), doi:10.1016/j.bbi.2016.02.020.

18. S. Leclercq, F. M. Mian, A. M. Stanisz, L. B. Bindels, E. Cambier, H. Ben-Amram, O. Koren, P. Forsythe, J. Bienenstock, Low-dose penicillin in early life induces long-term changes in murine gut microbiota, brain cytokines and behavior. *Nat. Commun.* **8**, 15062 (2017).

19. L. Desbonnet, G. Clarke, A. Traplin, O. O'Sullivan, F. Crispie, R. D. Moloney, P. D.

Cotter, T. G. Dinan, J. F. Cryan, Gut microbiota depletion from early adolescence in mice: Implications for brain and behaviour. *Brain. Behav. Immun.* **48**, 165–173 (2015).

20. J. R. Sheedy, R. E. H. Wettenhall, D. Scanlon, P. R. Gooley, D. P. Lewis, N. McGregor, D. I. Stapleton, H. L. Butt, K. L. DE Meirleir, Increased d-lactic Acid intestinal bacteria in patients with chronic fatigue syndrome. *In Vivo*. **23**, 621–8 (2009).

21. T. Arentsen, Y. Qian, S. Gkotzis, T. Femenia, T. Wang, K. Udekwu, H. Forssberg, R. Diaz Heijtz, The bacterial peptidoglycan-sensing molecule Pglyrp2 modulates brain development and behavior. *Mol. Psychiatry*. **22**, 257–266 (2017).

22. E. Wynendaele, F. Verbeke, S. Stalmans, B. Gevaert, Y. Janssens, C. Van De Wiele, K. Peremans, C. Burvenich, B. De Spiegeleer, Quorum sensing peptides selectively penetrate the blood-brain barrier. *PLoS One*. **10**, e0142071 (2015).

23. H. Fang, J. Kang, D. Zhang, Microbial production of vitamin B12: a review and future perspectives. *Microb. Cell Fact.* **16**, 15 (2017).

24. A. Pompei, L. Cordisco, A. Amaretti, S. Zanoni, D. Matteuzzi, M. Rossi, Folate production by bifidobacteria as a potential probiotic property. *Appl. Environ. Microbiol.* **73**, 179–85 (2007).

25. G. Li, K. D. Young, Indole production by the tryptophanase TnaA in Escherichia coli is determined by the amount of exogenous tryptophan. *Microbiology*. **159**, 402–10 (2013).

26. M. Matsumoto, R. Kibe, T. Ooga, Y. Aiba, E. Sawaki, Y. Koga, Y. Benno, Cerebral low-molecular metabolites influenced by intestinal microbiota: a pilot study. *Front. Syst. Neurosci.* **7**, 9 (2013).

27. E. Barrett, R. P. Ross, P. W. O'Toole, G. F. Fitzgerald, C. Stanton, γ-Aminobutyric acid production by culturable bacteria from the human intestine. *J. Appl. Microbiol.* **113**, 411–417 (2012).

28. Y. Asano, T. Hiramoto, R. Nishino, Y. Aiba, T. Kimura, K. Yoshihara, Y. Koga, N. Sudo, Critical role of gut microbiota in the production of biologically active, free catecholamines

548 in the gut lumen of mice. *AJP Gastrointest. Liver Physiol.* **303**, G1288–G1295 (2012).
549 29. S.-C. Hsu, K. R. Johansson, M. J. Donahue, The Bacterial Flora of the Intestine of
550 Ascaris suum and 5-Hydroxytryptamine Production. *J. Parasitol.* **72**, 545 (1986).
551 30. M. Lyte, Probiotics function mechanistically as delivery vehicles for neuroactive
552 compounds: Microbial endocrinology in the design and use of probiotics. *BioEssays*. **33**,
553 574–581 (2011).
554 31. C. S. Reigstad, C. E. Salmonson, J. F. Rainey, J. H. Szurszewski, D. R. Linden, J. L.
555 Sonnenburg, G. Farrugia, P. C. Kashyap, Gut microbes promote colonic serotonin
556 production through an effect of short-chain fatty acids on enterochromaffin cells. *FASEB*
557 *J.* **29**, 1395–403 (2015).
558 32. J. M. Yano, K. Yu, G. P. Donaldson, G. G. Shastri, P. Ann, L. Ma, C. R. Nagler, R. F.
559 Ismagilov, S. K. Mazmanian, E. Y. Hsiao, Indigenous bacteria from the gut microbiota
560 regulate host serotonin biosynthesis. *Cell*. **161**, 264–76 (2015).
561 33. J. X. Zhu, X. Y. Zhu, C. Owyang, Y. Li, Intestinal serotonin acts as a paracrine substance
562 to mediate vagal signal transmission evoked by luminal factors in the rat. *J. Physiol.* **530**,
563 431–42 (2001).
564 34. A. E. Hoban, R. D. Moloney, A. V. Golubeva, K. A. McVey Neufeld, O. O'Sullivan, E.
565 Patterson, C. Stanton, T. G. Dinan, G. Clarke, J. F. Cryan, Behavioral and neurochemical
566 consequences of chronic gut microbiota depletion during adulthood in the rat.
567 *Neuroscience* (2016), doi:10.1016/j.neuroscience.2016.10.003.
568 35. R. Janik, L. A. M. Thomason, A. M. Stanisz, P. Forsythe, J. Bienenstock, G. J. Stanisz,
569 Magnetic resonance spectroscopy reveals oral Lactobacillus promotion of increases in
570 brain GABA, N-acetyl aspartate and glutamate. *Neuroimage*. **125**, 988–995 (2016).
571 36. H. E. Hulme, L. M. Meikle, H. Wessel, N. Strittmatter, J. Swales, C. Thomson, A. Nilsson,
572 R. J. B. Nibbs, S. Milling, P. E. Andren, C. L. Mackay, A. Dexter, J. Bunch, R. J. A.
573 Goodwin, R. Burchmore, D. M. Wall, Mass spectrometry imaging identifies

palmitoylcarnitine as an immunological mediator during Salmonella Typhimurium infection. *Sci. Rep.* **7** (2017), doi:10.1038/s41598-017-03100-5.

37. A. Bouslimani, R. da Silva, T. Kosciolek, S. Janssen, C. Callewaert, A. Amir, K. Dorrestein, A. V. Melnik, L. S. Zaramela, J.-N. Kim, G. Humphrey, T. Schwartz, K. Sanders, C. Brennan, T. Luzzatto-Knaan, G. Ackermann, D. McDonald, K. Zengler, R. Knight, P. C. Dorrestein, The impact of skin care products on skin chemistry and microbiome dynamics. *BMC Biol.* **17**, 47 (2019).

38. R. A. Quinn, A. V. Melnik, A. Vrbanac, T. Fu, K. A. Patras, M. P. Christy, Z. Bodai, P. Belda-Ferre, A. Tripathi, L. K. Chung, M. Downes, R. D. Welch, M. Quinn, G. Humphrey, M. Panitchpakdi, K. C. Weldon, A. Aksenov, R. da Silva, J. Avila-Pacheco, C. Clish, S. Bae, H. Mallick, E. A. Franzosa, J. Lloyd-Price, R. Bussell, T. Thron, A. T. Nelson, M. Wang, E. Leszczynski, F. Vargas, J. M. Gauglitz, M. J. Meehan, E. Gentry, T. D. Arthur, A. C. Komor, O. Poulsen, B. S. Boland, J. T. Chang, W. J. Sandborn, M. Lim, N. Garg, J. C. Lumeng, R. J. Xavier, B. I. Kazmierczak, R. Jain, M. Egan, K. E. Rhee, D. Ferguson, M. Raffatellu, H. Vlamakis, G. G. Haddad, D. Siegel, C. Huttenhower, S. K. Mazmanian, R. M. Evans, V. Nizet, R. Knight, P. C. Dorrestein, Global chemical effects of the microbiome include new bile-acid conjugations. *Nature*. **579**, 1–19 (2020).

39. M. Shariatgorji, A. Nilsson, R. J. A. Goodwin, P. Källback, N. Schintu, X. Zhang, A. R. Crossman, E. Bezard, P. Svenningsson, P. E. Andren, Direct Targeted Quantitative Molecular Imaging of Neurotransmitters in Brain Tissue Sections. *Neuron*. **84**, 697–707 (2014).

40. N. Abbassi-Ghadi, E. A. Jones, K. A. Veselkov, J. Huang, S. Kumar, N. Strittmatter, O. Golf, H. Kudo, R. D. Goldin, G. B. Hanna, Z. Takats, Repeatability and reproducibility of desorption electrospray ionization-mass spectrometry (DESI-MS) for the imaging analysis of human cancer tissue: A gateway for clinical applications. *Anal. Methods* (2015), doi:10.1039/c4ay01770f.

41. T. Schramm, A. Hester, I. Klinkert, J. P. Both, R. M. A. Heeren, A. Brunelle, O. Laprévote, N. Desbenoit, M. F. Robbe, M. Stoeckli, B. Spengler, A. Römpp, ImzML - A common data format for the flexible exchange and processing of mass spectrometry imaging data. *J. Proteomics* (2012), doi:10.1016/j.jprot.2012.07.026.

42. G. Robichaud, K. P. Garrard, J. A. Barry, D. C. Muddiman, MSiReader: An open-source interface to view and analyze high resolving power MS imaging files on matlab platform. *J. Am. Soc. Mass Spectrom.* **24** (2013), pp. 718–721.

43. Allen Reference Atlases :: Atlas Viewer, (available at http://atlas.brain-map.org/).

44. Reference Atlas :: Allen Brain Atlas: Mouse Brain, (available at https://mouse.brain-map.org/static/atlas).

45. A. M. A. P. Fernandes, P. H. Vendramini, R. Galaverna, N. V. Schwab, L. C. Alberici, R. Augusti, R. F. Castilho, M. N. Eberlin, Direct Visualization of Neurotransmitters in Rat Brain Slices by Desorption Electrospray Ionization Mass Spectrometry Imaging (DESI - MS). *J. Am. Soc. Mass Spectrom.* **27**, 1944–1951 (2016).

46. M. Shariatgorji, N. Strittmatter, A. Nilsson, P. Källback, A. Alvarsson, X. Zhang, T. Vallianatou, P. Svenningsson, R. J. A. Goodwin, P. E. Andren, Simultaneous imaging of multiple neurotransmitters and neuroactive substances in the brain by desorption electrospray ionization mass spectrometry. *Neuroimage* (2016), doi:10.1016/j.neuroimage.2016.05.004.

47. H. Hulme, L. M. Meikle, N. Strittmatter, J. J. J. van der Hooft, J. Swales, R. A. Bragg, V. H. Villar, M. J. Ormsby, S. Barnes, S. L. Brown, A. Dexter, M. T. Kamat, J. C. Komen, D. Walker, S. Milling, E. K. Osterweil, A. S. MacDonald, C. J. Schofield, S. Tardito, J. Bunch, G. Douce, J. M. Edgar, R. A. Edrada-Ebel, R. J. A. Goodwin, R. Burchmore, D. M. Wall, Microbiome-derived carnitine mimics as previously unknown mediators of gut-brain axis communication. *Sci. Adv.* **6**, eaax6328 (2020).

48. D. S. Wishart, D. Tzur, C. Knox, R. Eisner, A. C. Guo, N. Young, D. Cheng, K. Jewell, D.

Arndt, S. Sawhney, C. Fung, L. Nikolai, M. Lewis, M. A. Coutouly, I. Forsythe, P. Tang, S. Shrivastava, K. Jeroncic, P. Stothard, G. Amegbey, D. Block, D. D. Hau, J. Wagner, J. Miniaci, M. Clements, M. Gebremedhin, N. Guo, Y. Zhang, G. E. Duggan, G. D. MacInnis, A. M. Weljie, R. Dowlatabadi, F. Bamforth, D. Clive, R. Greiner, L. Li, T. Marrie, B. D. Sykes, H. J. Vogel, L. Querengesser, HMDB: The human metabolome database. *Nucleic Acids Res.* (2007), doi:10.1093/nar/gkl923.

49. D. S. Wishart, Y. D. Feunang, A. Marcu, A. C. Guo, K. Liang, R. Vázquez-Fresno, T. Sajed, D. Johnson, C. Li, N. Karu, Z. Sayeeda, E. Lo, N. Assempour, M. Berjanskii, S. Singhal, D. Arndt, Y. Liang, H. Badran, J. Grant, A. Serra-Cayuela, Y. Liu, R. Mandal, V. Neveu, A. Pon, C. Knox, M. Wilson, C. Manach, A. Scalbert, HMDB 4.0: The human metabolome database for 2018. *Nucleic Acids Res.* (2018), doi:10.1093/nar/gkx1089.

50. M. Crumeyrolle-Arias, M. Jaglin, A. Bruneau, S. Vancassel, A. Cardona, V. Daugé, L. Naudon, S. Rabot, Absence of the gut microbiota enhances anxiety-like behavior and neuroendocrine response to acute stress in rats. *Psychoneuroendocrinology*. **42**, 207–217 (2014).

51. Y. E. Hoy, E. M. Bik, T. D. Lawley, S. P. Holmes, D. M. Monack, J. A. Theriot, D. A. Relman, Variation in Taxonomic Composition of the Fecal Microbiota in an Inbred Mouse Strain across Individuals and Time. *PLoS One*. **10**, e0142825 (2015).

52. D. Laukens, B. M. Brinkman, J. Raes, M. De Vos, P. Vandenabeele, Heterogeneity of the gut microbiome in mice: guidelines for optimizing experimental design. *FEMS Microbiol. Rev.* **40**, 117–32 (2016).

53. C. Alpert, S. Sczesny, B. Gruhl, M. Blaut, Long-term stability of the human gut microbiota in two different rat strains. *Curr. Issues Mol. Biol.* **10**, 17–24 (2008).

54. A. Mardinoglu, S. Shoaie, M. Bergentall, P. Ghaffari, C. Zhang, E. Larsson, F. Backhed, J. Nielsen, The gut microbiota modulates host amino acid and glutathione metabolism in mice. *Mol. Syst. Biol.* **11**, 834–834 (2015).

55. T. Kirschstein, F. Dammann, J. Klostermann, M. Rehberg, T. Tokay, R. Schubert, R. Köhling, “Dopamine induces contraction in the proximal, but relaxation in the distal rat isolated small intestine” (2009), , doi:10.1016/j.neulet.2009.08.080.

56. M. Donowitz, A. N. Charney, J. M. Heffernan, Effect of serotonin treatment on intestinal transport in the rabbit. *Am. J. Physiol. Metab.* **232**, E85 (1977).

57. R. Mazzoli, E. Pessione, The Neuro-endocrinological Role of Microbial Glutamate and GABA Signaling. *Front. Microbiol.* **7**, 1934 (2016).

58. M. Zareian, A. Ebrahimpour, F. A. Bakar, A. K. S. Mohamed, B. Forghani, M. S. B. Ab-Kadir, N. Saari, A glutamic acid-producing lactic acid bacteria isolated from Malaysian fermented foods. *Int. J. Mol. Sci.* **13**, 5482–97 (2012).

59. X. Lu, Z. Chen, Z. Gu, Y. Han, Isolation of γ-aminobutyric acid-producing bacteria and optimization of fermentative medium. *Biochem. Eng. J.* **41**, 48–52 (2008).

60. H. Uneyama, A. Niijima, A. San Gabriel, K. Torii, Luminal amino acid sensing in the rat gastric mucosa. *Am. J. Physiol. - Gastrointest. Liver Physiol.* **291** (2006).

61. L. Cynober, Metabolism of Dietary Glutamate in Adults. *Ann. Nutr. Metab.* **73**, 5–14 (2018).

62. L. Rivera-Calimlim, D. Hartley, D. Osterhout, Effects of ethanol and pantothenic acid on brain acetylcholine synthesis. *Br. J. Pharmacol.* **95**, 77–82 (1988).

63. S. Patassini, P. Begley, J. Xu, S. J. Church, N. Kureishy, S. J. Reid, H. J. Waldvogel, R. L. M. Faull, R. G. Snell, R. D. Unwin, G. J. S. Cooper, Cerebral Vitamin B5 (D-Pantothenic Acid) Deficiency as a Potential Cause of Metabolic Perturbation and Neurodegeneration in Huntington’s Disease. *Metabolites*. **9** (2019), doi:10.3390/METABO9060113.

64. E. D. Stein, J. M. Diamond, Do dietary levels of pantothenic acid regulate its intestinal uptake in mice? *J. Nutr.* **119**, 1973–83 (1989).

65. S. F. Rahman, M. R. Olm, M. J. Morowitz, J. F. Banfield, Functional potential of bacterial

strains in the premature infant gut microbiome is associated with gestational age. *bioRxiv*, 530139 (2019).

66. W. B. Bean, R. E. Hodges, K. Daum, J. T. Bradbury, R. Gunning, J. Manresa, W. Murray, P. Oliver, J. I. Routh, H. P. Schedl, M. Townsend, I. C. Tung, Pantothenic acid deficiency induced in human subjects. *J. Clin. Invest.* **34**, 1073–84 (1955).

67. J. Xu, S. Patassini, P. Begley, S. Church, H. J. Waldvogel, R. L. M. Faull, R. D. Unwin, G. J. S. Cooper, Cerebral deficiency of vitamin B5 (d-pantothenic acid; pantothenate) as a potentially-reversible cause of neurodegeneration and dementia in sporadic Alzheimer's disease. *Biochem. Biophys. Res. Commun.* **527**, 676–681 (2020).

68. M. Scholefield, S. J. Church, J. Xu, S. Patassini, N. M. Hooper, R. D. Unwin, G. J. S. Cooper, Substantively Lowered Levels of Pantothenic Acid (Vitamin B5) in Several Regions of the Human Brain in Parkinson's Disease Dementia. *Metabolites*. **11** (2021), doi:10.3390/METABO11090569.

69. R. Spector, C. E. Johanson, REVIEW: Vitamin transport and homeostasis in mammalian brain: focus on Vitamins B and E. *J. Neurochem.* **103**, 425–438 (2007).

70. R. Spector, B. Boose, Accumulation of Pantothenic Acid by the Isolated Choroid Plexus and Brain Slices In Vitro. *J. Neurochem.* **43**, 472–478 (1984).

71. C. G. Fernandes, M. S. da Rosa, B. Seminotti, P. Pierozan, R. W. Martell, V. L. Lagranha, E. N. B. Busanello, G. Leipnitz, M. Wajner, In vivo experimental evidence that the major metabolites accumulating in 3-hydroxy-3-methylglutaryl-CoA lyase deficiency induce oxidative stress in striatum of developing rats: A potential pathophysiological mechanism of striatal damage in this disorder. *Mol. Genet. Metab.* **109**, 144–153 (2013).

72. M. S. da Rosa, B. Seminotti, A. U. Amaral, C. G. Fernandes, J. Gasparotto, J. C. F. Moreira, D. P. Gelain, M. Wajner, G. Leipnitz, Redox homeostasis is compromised in vivo by the metabolites accumulating in 3-hydroxy-3-methylglutaryl-CoA lyase deficiency in rat cerebral cortex and liver. *Free Radic. Res.* **47**, 1066–75 (2013).

73. G. Leipnitz, B. Seminotti, A. U. Amaral, G. de Bortoli, A. Solano, P. F. Schuck, Â. T. S. Wyse, C. M. D. Wannmacher, A. Latini, M. Wajner, Induction of oxidative stress by the metabolites accumulating in 3-methylglutaconic aciduria in cerebral cortex of young rats. *Life Sci.* **82**, 652–662 (2008).

74. G. Leipnitz, B. Seminotti, C. G. Fernandes, A. U. Amaral, A. P. Beskow, L. de B. da Silva, Â. Zanatta, C. A. J. Ribeiro, C. R. Vargas, M. Wajner, Striatum is more vulnerable to oxidative damage induced by the metabolites accumulating in 3-hydroxy-3-methylglutaryl-CoA lyase deficiency as compared to liver. *Int. J. Dev. Neurosci.* **27**, 351–356 (2009).

75. N. West, K. Matiasek, C. Rusbridge, Olivopontocerebellar degeneration associated with 3-hydroxy-3-methylglutaric aciduria in a domestic shorthair cat: *https://doi.org/10.1177/20551169211037899*. **7** (2021), doi:10.1177/20551169211037899.

76. R. D. Semba, I. Trehan, X. Li, R. Moaddel, M. I. Ordiz, K. M. Maleta, K. Kraemer, M. Shardell, L. Ferrucci, M. Manary, Environmental Enteric Dysfunction is Associated with Carnitine Deficiency and Altered Fatty Acid Oxidation. *EBioMedicine*. **17**, 57–66 (2017).

77. S. N. Ukena, A. Singh, U. Dringenberg, R. Engelhardt, U. Seidler, W. Hansen, A. Bleich, D. Bruder, A. Franzke, G. Rogler, S. Suerbaum, J. Buer, F. Gunzer, A. M. Westendorf, Probiotic *Escherichia coli* Nissle 1917 inhibits leaky gut by enhancing mucosal integrity. *PLoS One*. **2**, e1308 (2007).

78. T. Nitta, M. Hata, S. Gotoh, Y. Seo, H. Sasaki, N. Hashimoto, M. Furuse, S. Tsukita, Size-selective loosening of the blood-brain barrier in claudin-5-deficient mice. *J. Cell Biol.* **161**, 653–660 (2003).

Figure Titles and Legends

Figure 1. Effects of the gut microbiome on neurotransmitters, neurotransmitter precursors and neurotransmitter metabolites in the murine brain and gut.

DESI-MS images of various DPP-derivatised neurotransmitters, neurotransmitter precursors or neurotransmitter metabolites in: (a) germ-free (GF) and specific-pathogen-free (SPF) mouse brains (N=5), (b) GF and SPF mice colons (N=4), (c) antibiotic treated (ABX) and untreated (Unt) mouse brains (N=5), and (d) ABX and Unt mice colons (N=5). H and E stained sections are shown, which are the same tissue sections that underwent DESI-MSI analysis. Tyrosine ([M+H]+ *m/z* 396.159), tryptophan ([M+H]+ *m/z* 419.175), dopamine ([M+H]+ *m/z* 368.165), glutamate ([M+H]+ *m/z* 362.139), serotonin ([M+H]+ *m/z* 391.181). The bar plots show the average metabolite abundance (ion intensity) across the whole tissue sections in the different groups tested. The bar plots for the brain also show relative abundance of neurotransmitters in multiple brain regions the cortex (cor), hippocampus (hipp), hypothalamus (hyp), thalamus (thal), striatum (stri), midbrain (mid), pons, medulla (med), white matter of the cerebellum (Cb white), grey matter of the cerebellum (Cb grey), the corpus callosum (cc) and the substantia nigra (SN). For (b), statistical analysis was performed using an unpaired t test. For (c) and (d), statistical analysis was performed using a paired t test, an unpaired t test or a Mann-Whitney U test where appropriate. For individual brain regions statistical analysis was performed using an unpaired t test. The *p* values were corrected for multiple testing by False Discovery Rate (FDR), two-stage step-up method. The desired FDR was set to 1%. The asterisks on the bar plot show significance with a *p* value of 0.01 (**), 0.001 (***), or ≤ 0.001 (****). Brain regions without asterisks were not significantly different in levels of neurotransmitter or metabolite. Error bars represent standard deviation. Scale bars = 2 mm. Ion images show target *m/z* ± 0.005Da.

Figure 2. Impact of the gut microbiome on 3-hydroxy-3-methylgularic acid levels in the gut and brain. DESI-MS images of HMG ([M-H]- *m/z* 161.045) in the (a) GF and SPF mouse brains (N=5), (b) GF and SPF mice colons (N=5), (c) ABX treated and Unt mouse brain (N=3),

and (d) ABX treated and Unt colons (N=3). H and E stained sections are shown, which are the same tissue sections that underwent DESI-MSI analysis. The bar plots show the average HMG abundance (ion intensity) across the whole tissue sections in the different groups tested. The bar plots for the brain also show relative abundance of neurotransmitters in multiple brain regions the cortex (cor), hippocampus (hipp), hypothalamus (hyp), thalamus (thal), striatum (stri), midbrain (mid), pons, medulla (med), white matter of the cerebellum (Cb white), grey matter of the cerebellum (Cb grey) and the corpus callosum (cc). Annotation in (a) Cb, cerebellum. Statistical analysis was performed using an unpaired t test. For individual brain regions statistical analysis was performed using an unpaired t test. The *p* values were corrected for multiple testing by False Discovery Rate (FDR), two-stage step-up method. The desired FDR was set to 1%. The asterisks on the bar plot show significance with a *p* value of 0.01 (**), 0.001 (***), or ≤ 0.001 (****). Brain regions without asterisks were not significantly different in levels of metabolite. Error bars represent standard deviation N=5. Scale bars=2 mm. Ion images show target *m/z* ± 0.005Da.

Figure 3. Effects of the gut microbiome on pantothenic acid (B5) levels in the gut and brain. DESI-MS images of B5 ([M-H]- *m/z* 218.103) in the (a) GF and SPF mouse brains (N=5), (b) GF and SPF mice colons (N=5), (c) ABX treated and Unt mouse brain (N=3), and (d) ABX treated and Unt colons (N=3). H and E stained sections are shown, which are the same tissue sections that underwent DESI-MSI analysis. The bar plots show the average B5 abundance (ion intensity) across the whole tissue sections in the different groups tested. The bar plots for the brain also show relative abundance of neurotransmitters in multiple brain regions the cortex (cor), hippocampus (hipp), hypothalamus (hyp), thalamus (thal), striatum (stri), midbrain (mid), pons, medulla (med), white matter of the cerebellum (Cb white), grey matter of the cerebellum (Cb grey) and the corpus callosum (cc). Annotation in (a) Cb, cerebellum; Hip, hippocampus; Hy, hypothalamus. Statistical analysis was performed using a paired t test. For individual brain

regions statistical analysis was performed using an unpaired t test. The *p* values were corrected for multiple testing by False Discovery Rate (FDR), two-stage step-up method. The desired FDR was set to 1%. The asterisks on the bar plot show significance with a *p* value of 0.01 (**), 0.001 (***), or ≤ 0.001 (****). Brain regions without asterisks were not significantly different in levels of metabolite. Error bars represent standard deviation N=5. Scale bars=2 mm. Ion images show target *m/z* ± 0.005Da.

Figures and Tables

Table 1 DESI-MSI parameters

Molecule	Pump solvent delivery	Spatial resolution	Ionisation mode	Mass range (*m/z)*	S-lens setting (V)	Mass resolution	Injection time (ms)
Neurotransmitters	1.5 µl/min	100 µm	Positive	200-800	75	35000	150
Pantothenic acid	1.5 µl/min	100 µm	Negative	65-400	50	70000	300
3-hydroxy-3-methylglutaric acid	1.5 µl/min	100 µm	Negative	65-400	50	70000	300

Figure 1

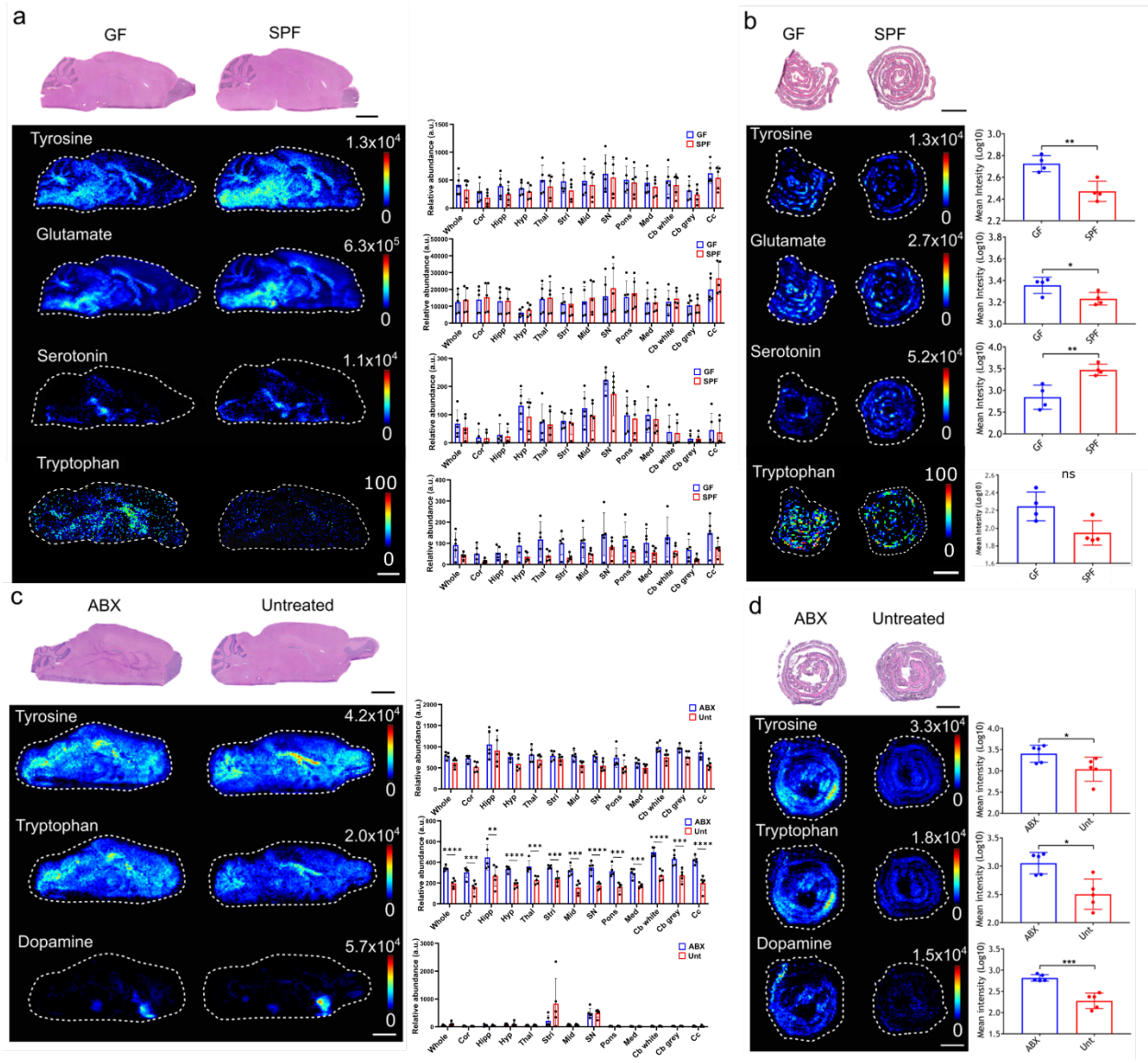
a
GF
SPF
Tyrosine
1.3x10^4
0
Glutamate
6.3x10^5
0
Serotonin
1.1x10^4
0
Tryptophan
100
0
Relative abundance (a.u.)
GF
SPF
Whole
Cor
Hipp
Hyp
Thal
Str
Mid
SN
Pons
Med
Cb white
Cb grey
Cc
b
GF
SPF
Tyrosine
1.3x10^4
0
Glutamate
2.7x10^4
0
Serotonin
5.2x10^4
0
Tryptophan
100
0
Mean Intesity (Log10)
**
*
**
ns
GF
SPF
c
ABX
Untreated
Tyrosine
4.2x10^4
0
Tryptophan
2.0x10^4
0
Dopamine
5.7x10^4
0
Relative abundance (a.u.)
ABX
Unt
****
***
**
*
d
ABX
Untreated
Tyrosine
3.3x10^4
0
Tryptophan
1.8x10^4
0
Dopamine
1.5x10^4
0
Mean intensity (Log10)
*
***
ABX
Unt

Figure 2

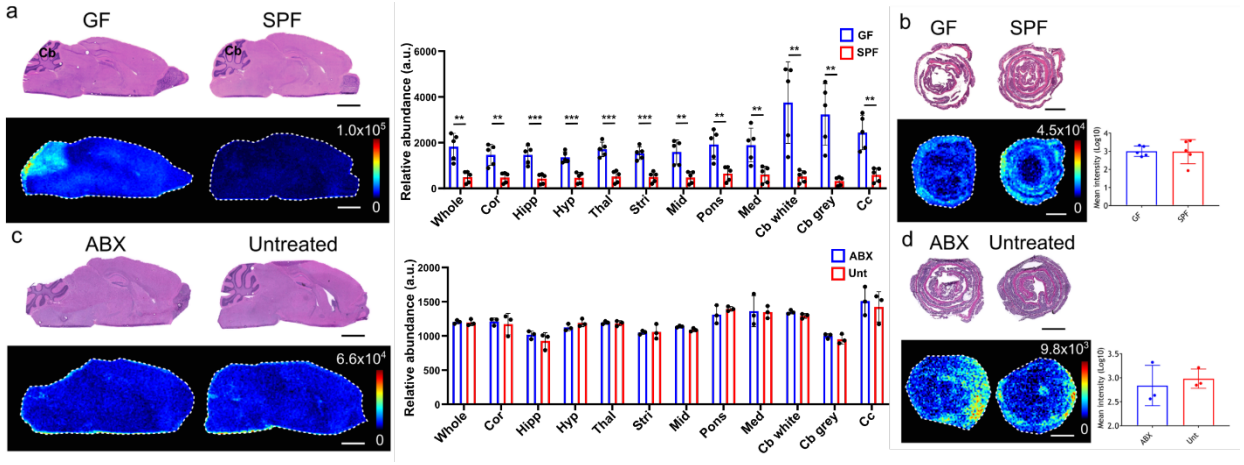

Figure 3

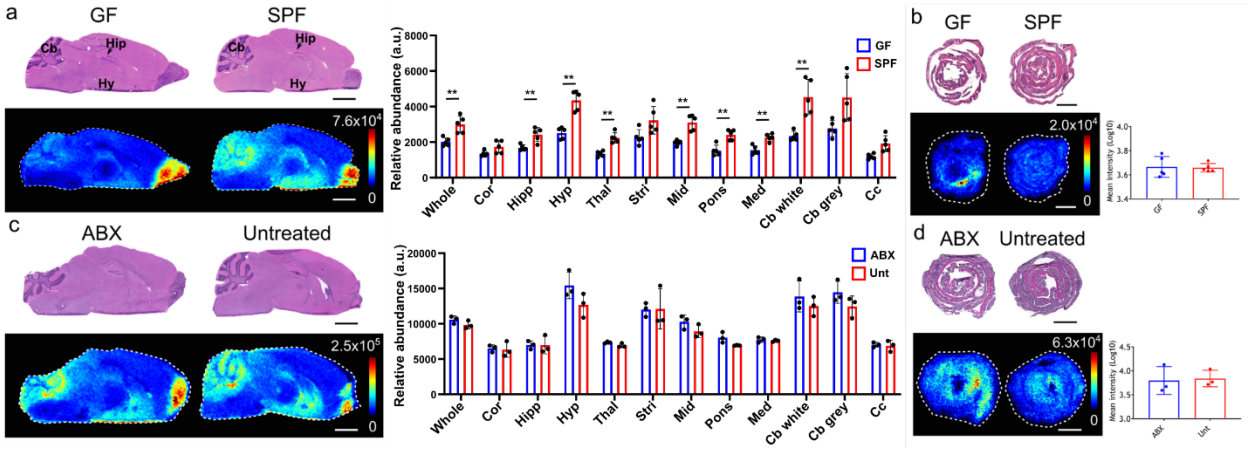

For Table of Contents Use Only

Mapping the influence of the gut microbiota on small molecules across the microbiome gut brain axis

Heather Hulme[1], Lynsey M. Meikle[1], Nicole Strittmatter[2], John Swales[2], Gregory Hamm[2], Sheila L. Brown[3], Simon Milling[1], Andrew S. MacDonald[3], Richard J.A. Goodwin[2], Richard Burchmore[1], Daniel M. Wall[1,*]

[1]Institute of Infection, Immunity and Inflammation, College of Medical, Veterinary and Life Sciences, Sir Graeme Davies Building, University of Glasgow, Glasgow G12 8TA, United Kingdom

[2]Imaging and Data Analytics, Clinical Pharmacology and Safety Sciences, Biopharmaceuticals R&D, AstraZeneca, Cambridge, CB4 0WG, UK

[3]Lydia Becker Institute of Immunology and Inflammation, Faculty of Biology, Medicine and Health, Manchester Academic Health Science Centre, University of Manchester, Manchester M13 9NT, UK

Caption: Mass spectrometry imaging of changes in concentration and localization of neurotransmitters and small molecules across the murine microbiome gut brain axis in response to microbiome presence or its perturbation by antibiotic treatment.